ACS APPLIED MATERIALS & INTERFACES

www.acsami.org

Research Article

Magnetic-Activated Cell Sorting Using Coiled-Coil Peptides: An Alternative Strategy for Isolating Cells with High Efficiency and Specificity

Meng-Jie Shen, René C.L. Olsthoorn, Ye Zeng, Thomas Bakkum, Alexander Kros,* and Aimee L. Boyle*

Cite This: *ACS Appl. Mater. Interfaces* 2021, 13, 11621−11630

Read Online

ACCESS | Metrics & More | Article Recommendations | Supporting Information

ABSTRACT: Magnetic-activated cell sorting (MACS) is an affinity-based technique used to separate cells according to the presence of specific markers. Current MACS systems generally require an antigen to be expressed at the cell surface; these antigen-presenting cells subsequently interact with antibody-labeled magnetic particles, facilitating separation. Here, we present an alternative MACS method based on coiled-coil peptide interactions. We demonstrate that HeLa, CHO, and NIH3T3 cells can either incorporate a lipid-modified coiled-coil-forming peptide into their membrane, or that the cells can be transfected with a plasmid containing a gene encoding a coiled-coil-forming peptide. Iron oxide particles are functionalized with the complementary peptide and, upon incubation with the cells, labeled cells are facilely separated from nonlabeled populations. In addition, the resulting cells and particles can be treated with trypsin to facilitate detachment of the cells from the particles. Therefore, our new MACS method promotes efficient cell sorting of different cell lines, without the need for antigen presentation, and enables simple detachment of the magnetic particles from cells after the sorting process. Such a system can be applied to rapidly developing, sensitive research areas, such as the separation of genetically modified cells from their unmodified counterparts.

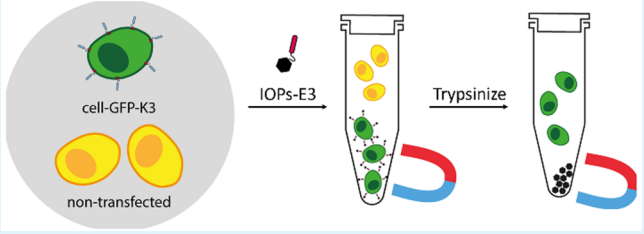

KEYWORDS: *magnetic-activated cell sorting, coiled-coil peptide, cell labeling, iron-oxide particles, cell separation*

INTRODUCTION

The sorting of specific cells from complex mixtures is necessary for a variety of applications, ranging from cancer research,[1−4] to assisted reproduction,[5] cell-based therapies,[6,7] and the selection of genetically modified cells.[8,9] Two of the primary affinity-based techniques used for cell sorting are fluorescence-activated cell sorting (FACS) and magnetic-activated cell sorting (MACS).[10,11] Although FACS has several advantages, including that analysis is rapid and multiple parameters can be simultaneously analyzed, the disadvantages include that fact that expensive, specialist equipment is needed and cells must be modified to display a fluorescent moiety. MACS can circumvent these disadvantages: no specialist equipment is required and no fluorescent labels are needed. Instead, MACS employs magnetic particles that can be functionalized to enable binding to a subset of cells in a mixture, facilitating separation.[12−15] Usually, the particles are functionalized with an antibody, which is specific for antigens expressed on the surface of cells of interest. The beads and the cells are incubated and subsequently placed in a magnetic field. Cells that do not express the antigen of interest are not retained in the magnetic field, whereas cells that do display the antigen of interest bind to the beads and are retained. Once the magnetic field is removed, the cells of interest can be eluted. However, MACS does have disadvantages: functionalization of the iron oxide particles (IOPs) with antibodies is not trivial, and such antibodies are typically expensive. Indeed, one study highlighted that, when MACS was used to select for induced pluripotent stem cells from a cell mixture, the antibody comprised 65% of the purification cost.[16] The MACS systems can also suffer from low cell purity after separation because of the nonspecific binding between the cells and the functionalized magnetic particles.[17,18] In addition, it is not trivial to separate the cells from the magnetic particles, which can lead to adverse effects. For example, magnetic particles can influence the phenotype and function of some cells,[19,20] in addition to affecting cell viability.[21,22]

Therefore, there is a need to design and synthesize functionalized magnetic particles that possess a high specificity for the cells of interest and are facile to dissociate from the cells after separation. Such a system would benefit multiple areas of cell biology and medicine, for example facilitating the separation, and subsequent enrichment, of genetically modified cells.

Received: December 15, 2020
Accepted: February 22, 2021
Published: March 3, 2021

https://dx.doi.org/10.1021/acsami.0c22185
ACS Appl. Mater. Interfaces 2021, 13, 11621−11630

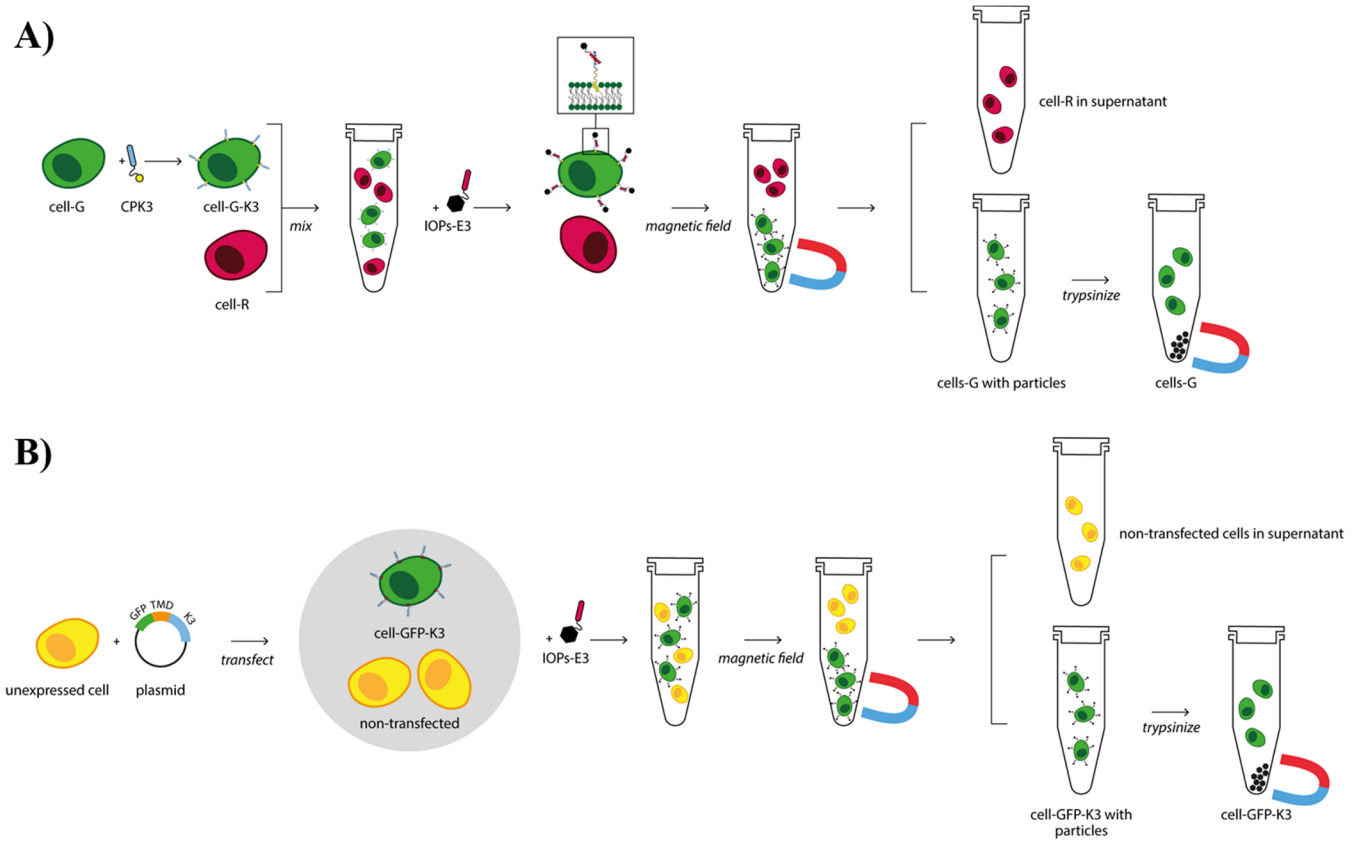

Figure 1. Coiled-coil-based MACS. Cells are either (A) functionalized with a coiled-coil forming peptide or (B) transfected with a K_3-containing plasmid; low transfection rates mean not all cells express the K_3 peptide. IOPs bearing the complementary peptide are added and separation is facilitated by coiled-coil formation and application of a magnetic field. Postseparation, cells are separated from the IOPs via trypsinization.

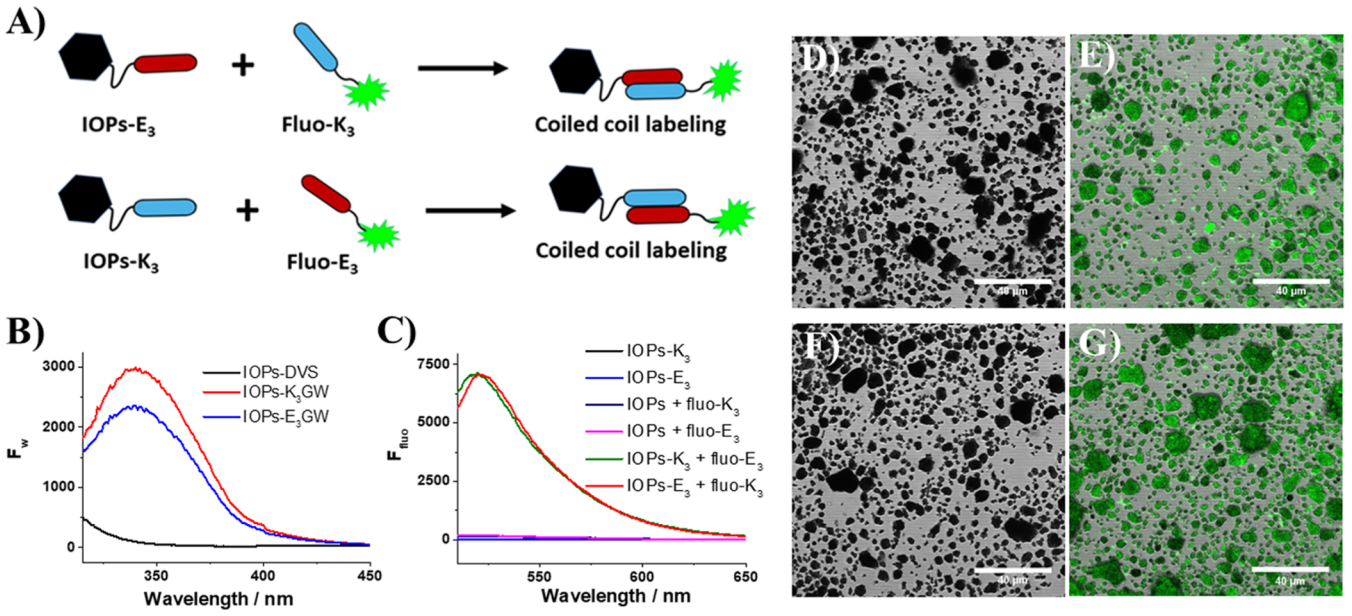

Figure 2. Coiled-coil-functionalized magnetic particles. (A) Schematic of fluorescent labeling of the IOPs: coiled-coil functionalized IOPs are incubated with the complementary fluorescent peptide. (B) Tryptophan fluorescence spectrum of functionalized IOPs, indicating attachment of the peptides to the particles. (C) Fluorescein fluorescence spectrum of fluorescently labeled IOPs; a fluorescein spectrum is only observed when the IOPs are labeled with the complementary peptide. (D–G) Confocal microscopy images of: IOP-DVS treated with (D) fluo-K_3, (E) IOP-E_3 treated with fluo-K_3; (F) IOP-DVS treated with fluo-E_3; and (G) IOP-K_3 treated with fluo-E_3. Scale bar: 40 μm.

Coiled coils are a protein-folding motif comprising two or more alpha-helices that interact to form a left-handed supercoil.[23] Different oligomer states, orientations of helices, and both homomeric and heterodimeric assemblies are possible.[24] Moreover, rules exist for the programmable design of such structures,[25,26] which has enabled synthetic coiled-coil systems

https://dx.doi.org/10.1021/acsami.0c22185
ACS Appl. Mater. Interfaces 2021, 13, 11621−11630

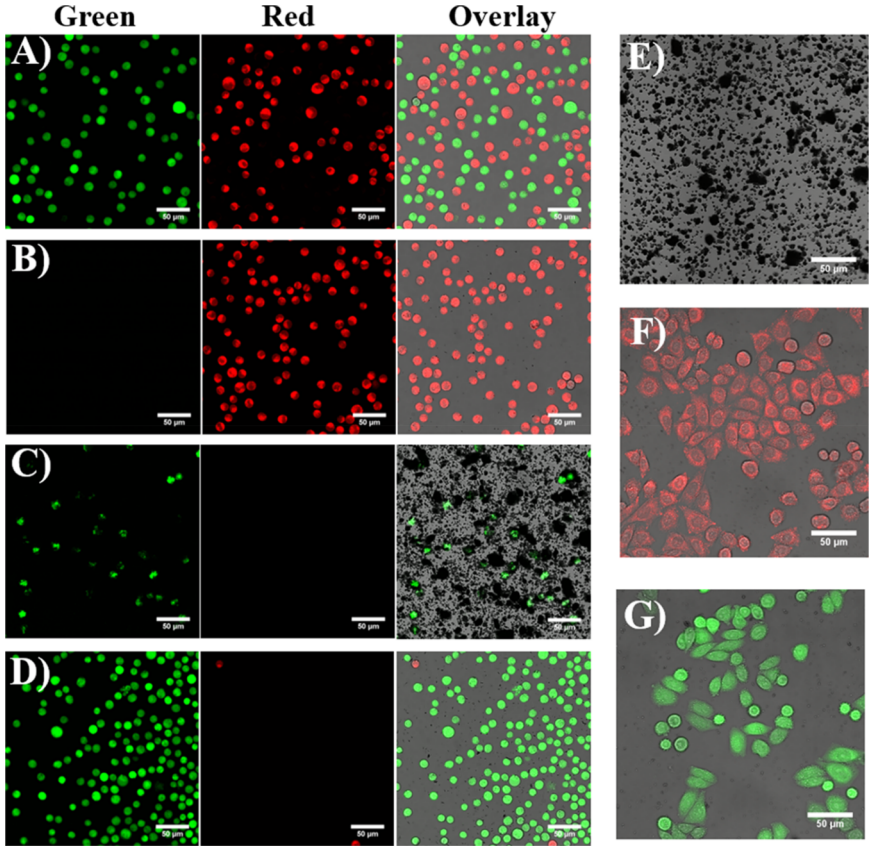

Figure 3. Coiled-coil-facilitated MACS of HeLa cells. (A) CPK_3-modified HeLa cells stained with CellTracker Green mixed with nonfunctionalized HeLa cells stained with CellTracker Red; (B) cells in the supernatant after MACS; (C) IOP-attached cells after MACS; (D) cells detached from the IOPs after trypsinization; (E) no visible cells remain attached to the IOPs after trypsinization; (F) cells from the supernatant and (G) those detached from IOPs show signs of recovery and growth after 24 h. Scale bar: 50 μm.

to be designed and employed in a variety of applications.[27−30] We were motivated to determine whether coiled-coil peptides could be used to separate cells in a MACS-based approach. Therefore, we designed a MACS system based on interactions between magnetic beads and cells that were functionalized with complementary coiled-coil forming peptides (Figure 1). We employed a heteromeric coiled-coil system, dubbed E_3/K_3.[31] Nanometer-sized iron oxide magnetic particles (IOPs) were coated with dextran-divinyl sulfone (dextran-DVS) and subsequently functionalized with E_3 to yield IOP-E_3. HeLa, CHO, and NIH3T3 cells were incubated with a lipidated K_3 derivative (CPK_3), which is known to spontaneously incorporate into the cell membrane.[32] When the cells and the functionalized IOPs were mixed, cells that displayed K_3 on their surface bound to the IOP-E_3 via the formation of a coiled-coil. Subsequent application of an external magnetic field facilitated isolation of these cells with high efficiency and specificity (Figure 1A). Another advantage of this system is that the coiled-coil peptides could be degraded by trypsin, which made the dissociation of the cells from the IOPs facile and efficient. We subsequently demonstrate that HeLa, NIH3T3, and CHO cells can be transfected with a plasmid containing K_3. These cells express K_3 on their membrane and we show that these cells could be separated (Figure 1B), and subsequently enriched, from nontransfected cells. These results demonstrate that our coiled-coil based MACS system can facilitate cell separation, and subsequent enrichment of transfected cells, with high specificity and efficiency.

RESULTS AND DISCUSSION

Design and Synthesis of Peptide-Functionalized IOPs.

Functionalized magnetic particles suitable for cell sorting need to possess several properties including specificity for the cells of interest, high binding and separation efficiency, and effective dissociation. To fulfill these criteria, we designed a coiled-coil-functionalized IOP system. Two complementary peptides known as K_3 ($(KIAALKE)_3$) and E_3 ($(EIAALEK)_3$), named for the prevalence of lysine and glutamic acid residues in their respective sequences, were employed.[31] These two peptides interact to form a heterodimeric coiled coil with a micromolar dissociation constant. This tight binding enables peptide-functionalized IOPs to bind to the complementary peptide with high efficiency (Figure 2A).

IOPs need to be coated to reduce nonspecific interactions with cells and to facilitate functionalization with a moiety specific to the cells of interest. In this study, IOPs were synthesized and coated with a dextran-divinyl sulfone (Dex-DVS) polymer in a one-pot reaction. The DVS functionality facilitates labeling of the IOPs with any compound containing a free sulfhydryl group via a Michael addition. An added advantage is that the number of DVS groups can be adjusted by synthesizing Dex-DVS with differing degrees of substitution, allowing for control over the number of functional groups displayed on the surface of the IOPs.

Conjugation of the coiled-coil forming peptides to the IOPs was facilitated by modifying the peptides to include a free sulfhydryl group. To this end, Ac-E_3GW-PEG_4-Cys and Ac-

https://dx.doi.org/10.1021/acsami.0c22185
ACS Appl. Mater. Interfaces 2021, 13, 11621−11630

Table 1. FACS Quantification of Cell Populations before and after MACS

	before MACS (%)		after MACS:supernatant (%)		after MACS:detached cells (%)	
cell line	red	green	red	green	red	green
HeLa	51.5	47.2	99.2 (0.2)[a]	0.5 (0.2)	4.9 (1.5)	94.8 (1.3)
CHO	44.5	55	99.7 (0.0)	0.3 (0.0)	4.3 (0.1)	95.7 (0.1)
NIH3T3	48.5	51.5	100 (0.0)	0 (0.0)	0.7 (0.2)	99.3 (0.2)

[a]Error is calculated as the standard deviation from the average of at least two independent measurements.

K_3GW-PEG$_4$-Cys were designed. These peptides incorporate a cysteine (Cys, C) at their C-terminus. A polyethylene glycol (PEG) spacer was included between the cysteine and the rest of the peptide sequence to minimize potential steric hindrance, which may impact coiled-coil formation. A tryptophan (Trp, W) was included to facilitate detection and quantification of the peptide.

To demonstrate the peptide-functionalized IOPs were successfully synthesized, we employed fluorescence spectroscopy. IOPs functionalized with the coiled-coil forming peptides exhibit a fluorescence spectrum corresponding to that of Trp (Figure 2B), which indicates the peptides were successfully conjugated to the IOPs.

Coiled-coil formation was subsequently confirmed using a fluorescence labeling assay. The fluorescein conjugated peptides, fluo-K_3 and fluo-E_3, were mixed with either non-functionalized IOPs or IOPs bearing the complementary peptide. Figure 2C shows that a fluorescein fluorescence spectrum is only observed when the peptides are mixed with IOPs functionalized with the complementary peptides. This indicates coiled-coil formation and demonstrates that no nonspecific binding between fluo-E_3 or fluo-K_3 and non-functionalized IOPs occurs. The results were verified by confocal microscopy imaging (Figure 2D–G). The unmodified IOPs did not exhibit fluorescence after incubation with fluo-K_3 or fluo-E_3 (Figure 2D, F), whereas peptide-modified IOPs have a green fluorescent surface after labeling with the complementary peptide, i.e., IOP-E_3 + fluo-K_3 (Figure 2E) or IOP-K_3 + fluo-E_3 (Figure 2G).

MACS for Lipopeptide-Decorated Cells. We have previously employed the lipopeptides CPK and CPE to facilitate membrane fusion.[33,34] These lipopeptides comprise the K and E peptides, with a PEG spacer that connects the peptide to a cholesterol anchor. This anchor enables the insertion of the lipopeptide into the lipid bilayer of a cell membrane. By functionalizing specific cells with these lipopeptides and adding IOPs functionalized with the complementary coiled-coil forming peptide, cells can be separated from others in a mixture.

To confirm that the lipopeptides synthesized for this study are capable of inserting into the cell membrane and subsequently forming a coiled coil, we performed a cell membrane labeling assay . The fluo-K_3 or fluo-E_3 peptides were added to cells decorated with the complementary lipopeptide. Using confocal microscopy, it was determined that the lipopeptide-decorated cells exhibited a fluorescently labeled membrane, whereas no fluorescent labeling was observed on nondecorated cell membranes (Figure S1).

After it was confirmed that coiled-coil forming peptides could be used to functionalize IOPs and cell membranes and that coiled-coil formation occurred, a proof-of-principle coiled-coil-mediated MACS experiment was designed. Separate HeLa cell populations were stained with either CellTracker Green or CellTracker Red. Green cells were incubated with CPK$_3$ for 1 h, before being mixed with the same number of red cells. IOP-E_3 were subsequently added to the cell mixture. It was anticipated that the IOP-E_3 would selectively bind to the CPK$_3$-decorated green cells via coiled-coil formation. Through the application of an external magnetic field, cells attached to the magnetic particles could be isolated. The IOP-attached cells could subsequently be treated with trypsin to dissociate the magnetic particles before an external magnetic field could again be used to separate the IOPs from the detached HeLa cells.

Confocal imaging was performed directly after MACS; the results are shown in Figure 3. Before MACS, the cell population contained CPK$_3$-decorated green cells and undecorated red cells (Figure 3A). After MACS, only red cells were found in the supernatant (Figure 3B) and cells attached to the IOPs were almost exclusively green (Figure 3C). This demonstrates that the K_3/E_3 coiled-coil-based MACS system can be used to efficiently separate cell populations. To demonstrate that the cells can be cleaved from the IOPs, we incubated them with trypsin and then separated from the IOPs using an external magnetic field. Figure 3D shows the image of the cells after dissociation: most of the cells exhibit green fluorescence. The cell-IOP dissociation is efficient: no cells were observed to remain attached to the IOPs (Figure 3E). After MACS, the cells were allowed to grow for 24 h before imaging again to demonstrate that both the cells from the supernatant (Figure 3F) and the cells detached from the IOPs (Figure 3G) remain viable. The same study was then performed using CHO and NIH3T3 cells to illustrate the broad applicability of this MACS system (Figures S2 and S3).

Although confocal imaging provides a qualitative impression of the efficiency of this system, quantification of cell separation is desirable. Therefore, flow cytometry was employed for all three cell lines. Before MACS, the flow cytometry data shows the cells are mixed in an approximately 1:1 ratio, as designed, Table 1. After one round of MACS, the cells were demonstrated to be highly efficiently separated as, for all three cells lines tested, more than 99% of the cells in the supernatant were red cells and more than 94% of cells detached from the IOPs were green cells (Table 1, Figures S4–S6).

Alternative IOP Functionalization. Cell membranes are usually negatively charged. For this reason, IOPs were functionalized with E_3 and not K_3, as it was hypothesized that IOP-K_3 could nonspecifically interact with the negatively charged cell membrane. To verify this hypothesis, an experiment was performed using HeLa cells modified with CPE$_3$ and IOPs functionalized with K_3 (Figure S7). The CPE$_3$-decorated green cells were mixed with red cells in a 1:1 ratio (Figure S7A). The cell mixture was incubated with IOP-K_3 and after MACS, only red cells were found in the supernatant (Figure S7B). However, a mixture of red and green cells were found to be attached to the IOPs (Figures S7C); this is more evident after trypsinization (Figure S7D). In addition, FACS analysis was performed and this revealed that the cells detached from the IOPs have almost equal populations of green and red cells (Figures S7E and S8).

https://dx.doi.org/10.1021/acsami.0c22185
ACS Appl. Mater. Interfaces 2021, 13, 11621–11630

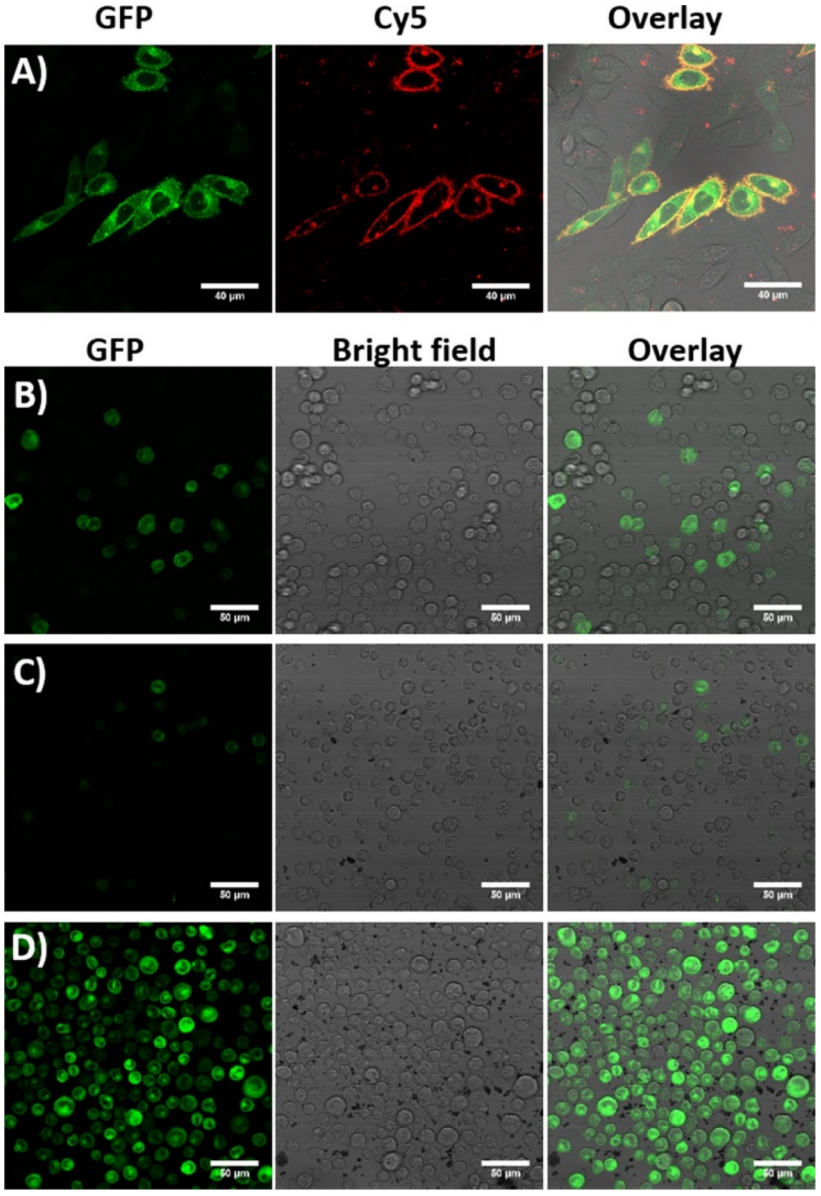

Figure 4. HeLa cell membrane labeling and cell sorting. (A) HeLa cells were transfected with a plasmid containing the K_3-TMD-GFP gene. The transfected cells were subsequently incubated with Cy5-E_3 to demonstrate successful expression of K_3 at the cell surface. Green channel, GFP; red channel, Cy5. Scale bar: 40 μm. Transfected cells were then subjected to MACS: (B) before MACS; (C) cells from the supernatant after MACS; (D) cells detached from IOPs after MACS. Green channel: GFP. Scale bar: 50 μm.

Combined, these experiments reveal that coiled-coil-forming peptide-functionalized IOPs can be used to efficiently sort cells bearing the complementary coiled-coil-forming peptide from a mixture. This system can be applied to a variety of different cell lines. These data also indicate that the charge of the peptide that is conjugated to the IOPs makes a significant difference to the efficiency of the cell sorting process.

MACS with GFP-K_3-Expressed Cells. For the proof-of-principle experiment, cells have to be manually decorated with K_3 before cell sorting; this process limits the potential applications of the MACS system. To fully benefit from using coiled coils as a cell-surface marker, cells that express K_3 on their membranes were employed (Figure 1B): such a system has been used previously in our lab.[34] The K_3 peptide was fused to a signal sequence and a transmembrane domain (TMD) from the platelet-derived growth factor receptor beta (PDGFRB). The presence of this signaling sequence and the TMD ensures that the K_3 peptide is transported to, and anchored in, the cell membrane. In addition, GFP was included to act as a fluorescent marker to illustrate expression of the K_3-TMD-GFP construct after transfection. GFP can also be used as a fluorescent label for FACS quantification before and after MACS.

After cell transfection and 2 weeks of antibiotic selection, approximately 10% of all transfected cells successfully expressed the K_3-TMD-GFP construct. A cell-labeling experiment was subsequently performed using a Cy5-conjugated E_3 peptide to confirm that the K_3 peptide was successfully expressed on the cell membrane (Figure 4A).

As the K_3 peptide was indeed expressed on the cell membrane, it was possible to use it as a selection marker for cell sorting. As GFP is coexpressed in the K_3-expressing cells, confocal microscopy can be employed to track the cell sorting process. Before MACS, a low percentage of green cells were found in the cell mixture because of the low transfection efficiency (Figure

https://dx.doi.org/10.1021/acsami.0c22185
ACS Appl. Mater. Interfaces 2021, 13, 11621−11630

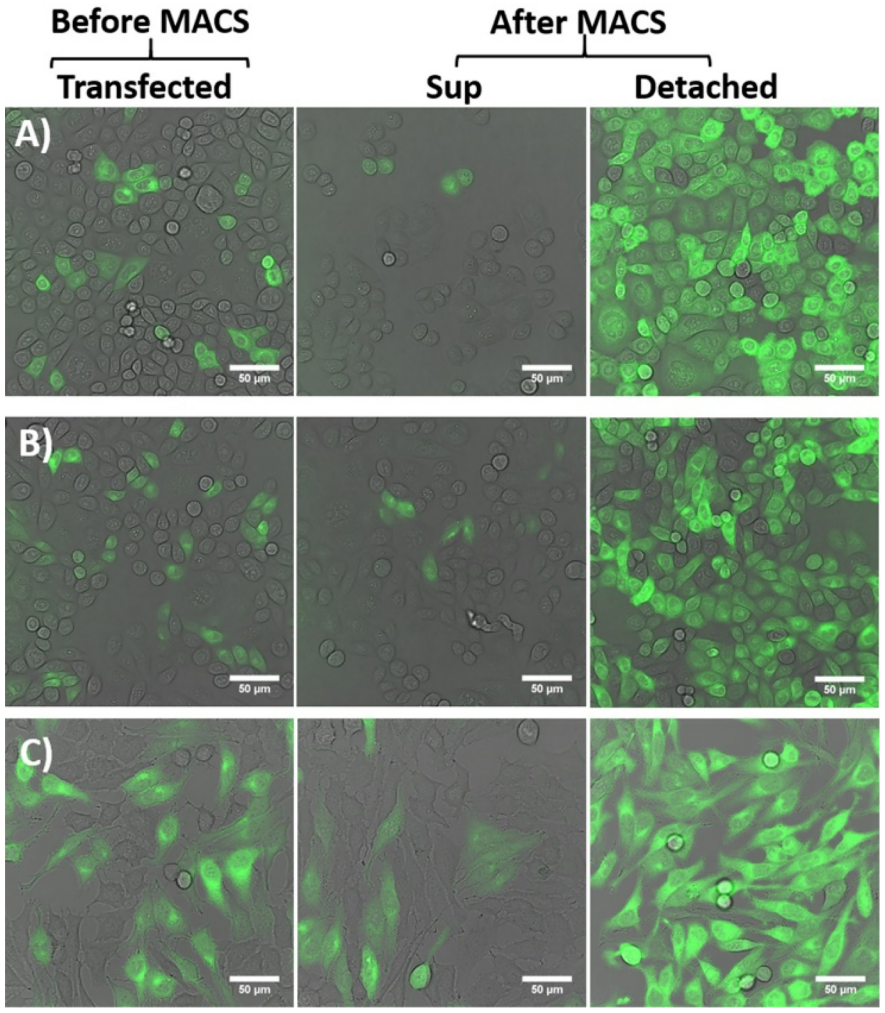

Figure 5. Imaging of K_3-TMD-GFP cells before and after MACS. (A) HeLa-K_3 cells, (B) CHO-K_3 cells, (C) NIH3T3-K_3 cells. The left column shows transfected cells before MACS, the middle column shows cells in the supernatant after MACS and cells detached from IOPs after MACS are on the right. All images are an overlay of bright-field and fluorescence microscopy images. Scale bar: 50 μm.

4B). IOP-E_3 were added to the cells and an external magnetic field was applied. After MACS, few green cells were observed in the supernatant (Figure 4C), whereas cells retained in the magnetic field and then detached from the IOPs were GFP-expressing cells (Figure 4D). This shows that the coiled-coil peptide-based MACS system is capable of selective separation of K_3-expressing cells from nontransfected cells. Although some cells that expressed GFP were found in the supernatant, the fluorescence level was low, indicating that the expression level of K_3 could also affect the separation. The cells were subsequently cultured for 2 days: Figure 5A shows that the GFP-positive cells could be enriched to a high level after coiled-coil-based MACS. FACS quantification showed only 17.4% of GFP positive cells in the transfected cell mixture before MACS (Table 2, and Figure S9), but after MACS selection, 94.3% of GFP-positive cells were obtained. These results confirm that GFP-K_3 expressed cells can be effectively enriched by this MACS system.

To demonstrate the wider applicability of the transfected MACS system for cell sorting and enrichment, we again employed CHO and NIH3T3 cell lines (Figure 5B, C). Cells were analyzed using FACS after separation (Figures S10 and 11). For CHO cells, an enrichment from 14.8 to 76% of GFP-expressing cells could be obtained after MACS. This system is even more successful for NIH3T3 cells; the FACS data show that 24.2% of GFP-K_3 expressing NIH3T3 cells could be enriched to 95.6% after MACS.

Table 2. FACS Quantification of GFP Positive Cells before and after MACS

		after MACS (%)	
cell line	before MACS (%)	supernatant	detached
HeLa	17.4	11.7 (0.6)[a]	94.3 (2.2)
CHO	14.8	12.2 (8.1)	76.0 (2.5)
NIH3T3	24.2	19.8 (0.1)	95.6 (0.4)

[a]Errors are calculated as the standard deviation from the average of at least two independent measurements.

Both the qualitative and quantitative data show that the GFP-K_3 expressing cells from different cell lines can be efficiently isolated from a cell mixture using IOP-E_3. These results demonstrate that the coiled-coil-mediated MACS system can be applied to enrich cell populations. For this study, GFP was coexpressed with K_3 to facilitate both imaging and quantification by FACS. However, MACS itself does not require the cells to express GFP or indeed any fluorophore, which is beneficial for studies where fluorescent proteins are detrimental and therefore FACS is not possible. Additionally, the GFP could be replaced by any protein of interest and a single round of coiled-coil-

https://dx.doi.org/10.1021/acsami.0c22185
ACS Appl. Mater. Interfaces 2021, 13, 11621−11630

mediated MACS will separate the cells expressing this protein with high specificity and efficiency.

CONCLUSIONS

In this study, we have taken advantage of coiled-coil peptide interactions and designed a new MACS system based on this noncovalent interaction. This MACS system facilitates efficient, facile cell sorting. A particularly attractive feature of this system is that the isolated cells can be easily dissociated from the IOPs by trypsinization, meaning the magnetic particles do not remain attached to the cells. This system may not be suitable for all cell types, particularly those isolated from tissues, because of the need to incorporate an extrinsic selection marker. However, the fact that the K_3 peptide can be employed as a selection marker for transfected cells means that this approach has the potential to become an alternative method for transfected cell selection, eliminating the need for FACS or antibiotics. Moreover, the plasmid can be modified to include any gene of interest, either as a fusion with K_3 or by including cleavage sites. Such a system could therefore have applications in a wide range of biomedical areas that require cell separation.

EXPERIMENTAL SECTION

Chemicals. All chemicals were purchased from Sigma unless otherwise stated. Amino acids and HCTU were purchased from Novabiochem. Tentagel HL RAM resin was purchased from Iris Biotech GmbH. Piperidine, trifluoroacetic acid, acetic anhydride, and all other solvents were purchased from Biosolve. Oxyma pure was purchased from Carl Roth GmbH. Dextran 70 was supplied by Pharmacosmos. CellTracker Red and Green, lipofectamine 3000, and 2 kDa MWCO dialysis membrane were purchased from Thermo Fisher. Confocal chambered coverslips (μ-Slide 8 Well) were purchased from Ibidi. All cell culture supplies were purchased from Starstedt. Carbon/Formvar grids for transmission electron microscopy were purchased from Agar Scientific.

Peptide Synthesis. For the synthesis of CPE_3 and CPK_3, peptides K_3 ($(KIAALKE)_3$) and E_3 ($(EIAALEK)_3$) were synthesized using Fmoc chemistry on a CEM Liberty Blue microwave-assisted peptide synthesizer. DIC was used as the activator and Oxyma as the activator base. Fmoc deprotection was performed with 20% piperidine in DMF. The peptide was synthesized on a Tentagel HL RAM resin (0.39 mmol/g). Once synthesis of the peptide was complete, 2 equiv. of N_3-PEG_4-COOH (synthesized as described elsewhere),[35] were manually coupled to the peptides on resin, using 3 equiv. of HCTU and 5 equiv. of DIPEA in DMF. The resin was washed with DMF after 3 h. Five equivalents of trimethylphosphine (1 M in toluene) in a dioxane:H_2O (6:1) mixture were added to the resin to reduce the azide. After 3 h, the resin was washed with dioxane followed by DMF before cholesteryl hemisuccinate (3 equiv.) was coupled to the N-terminus of the PEG linker using 3 equiv. of HCTU and 5 equiv. of DIPEA in DMF. After overnight coupling, the resin was washed with DMF followed by DCM and the resulting CPK_3 or CPE_3 construct was cleaved from the resin by adding 5 mL of a TFA:triisopropylsilane (97.5:2.5%) mixture and shaking for 45 min. The crude peptide was precipitated by pouring into 45 mL of cold diethyl ether and isolated by centrifugation. The peptide pellet was dissolved in 20 mL of H_2O with 10% acetonitrile and freeze-dried to yield a white powder.

The fluo-E_3 and fluo-K_3 peptides were synthesized in a similar manner. Two additional glycine residues were coupled to the N-terminus of the K_3 and E_3 peptides. 5(6)-Carboxyfluorescein (3 equiv.) was subsequently manually coupled to the peptides using four equiv. HCTU and 6 equiv. of DIPEA in DMF. After an overnight reaction, the resin was washed using DMF and the fluorophore-labeled peptides, flu-K_3 and flu-E_3, were cleaved from the resin using 5 mL of TFA:triisopropylsilane:H_2O (95%:2.5%:2.5%) for 1 h. The peptide was precipitated into diethyl ether, centrifuged, redissolved in H_2O and MeCN, and freeze-dried.

For the Ac-E_3GW-PEG_4-Cys and Ac-K_3GW-PEG_4-Cys peptides, cysteine was coupled to Tentagel HL RAM resin before N_3-PEG_4-COOH was coupled to the cysteine using the procedure described above. After 3 h, the resin was washed and the azide reduced. The resin was transferred to the peptide synthesizer and either E_3 ($(EIAALEK)_3$GW) or K_3 ($(KIAALKE)_3$GW) was synthesized. Upon completion of the synthesis, the resin was manually acetylated by adding 3 mL of an acetic anhydride:pyridine:DMF (5%:6%:89%) solution. After 1 h, the resin was washed with DMF and DCM, before the peptide was cleaved from the resin by adding 5 mL of TFA:TIPS:EoDT:H_2O (92.5:2.5%:2.5%:2.5%). After 2 h, the peptide was precipitated into diethyl ether, centrifuged, redissolved, and freeze-dried.

Cy5-E_3 was synthesized for labeling GFP-K_3 expressing cells. E_3 was synthesized using the method described above. After the synthesis, 3 equiv. of 4-pentynoic acid, 4 equiv. of HCTU and 6 equiv. of DIPEA in 2 mL of DMF were added to the E_3 peptide, on the resin, to facilitate coupling of an alkyne to the N-terminus. After 1 h, the resin was washed (DMF followed by DCM) and the peptide was cleaved. The alkyne-E_3 peptide was purified using HPLC (see below) before coupling to azide-Cy5. This coupling was performed by dissolving 1.55 mg (9.7 nmol) of $CuSO_4$ in 1 mL of H_2O. Nineteen milligrams (97 nmol) of L-ascorbic acid was subsequently added and the color of the solution became brown, before turning light yellow. Twenty-one milligrams (48.5 nmol) of tris(3-hydroxypropyltriazolylmethyl)amine was dissolved in 150 μL of DMSO and added to solution, which was stirred for 3 min at 500 rpm before 1 mg (0.97 nmol) of azide-Cy5 in 500 μL of H_2O was added, followed by 11.5 mg (4.85 nmol) of alkyne-E_3 in 500 μL of H_2O. The reaction was stirred for 2 h before being dialyzed overnight using a 2 kDa MWCO membrane. The resulting Cy5-E3 peptide was purified using HPLC.

Peptide Purification. Peptide and lipopeptide purification was performed using reversed-phase HPLC on a Shimazu system with two LC-8A pumps and an SPD-20A UV−vis detector.

Lipopeptide (CPK_3 and CPE_3) purification was performed with a Vydac C4 column (22 mm diameter, 250 mm length, 10 μm particle size). A linear gradient from 20 to 80% acetonitrile (with 0.1% TFA) in water (with 0.1% TFA) was performed over 36 min, with a flow rate of 12 mL/min.

Peptides Ac-K_3GW-PEG_4-Cys, Ac-K_3GW-PEG_4-Cys, fluo-E_3, fluo-K_3, E_3, and Cy5-E_3 were purified using a Kinetix Evo C18 column (21.2 mm diameter, 150 mm length, 5 μm particle size). A linear gradient from 20 to 55% acetonitrile (with 0.1% TFA) and water (0.1% of TFA) was used for the HPLC method: the running time was 28 min, and the flow rate was 12 mL/min.

After purification, the collected fractions of all lipopeptides and peptides were assessed using LC-MS (Figures S12−S15, Table S1). Fractions that were deemed to be >95% pure were combined and lyophilized.

Modification of Dextran with DVS. The synthesis of dextran-DVS was performed according to a previously reported protocol.[36] Briefly, 10 g (61.7 mmol) of dextran 70 was dissolved in 300 mL of a 0.1 M NaOH solution in an ice bath. Afterward, 23 mL (229 mmol) of divinyl sulfone was added under vigorous stirring (1000 rpm). The reaction was left for 65 s before 5 mL of 6 M HCl was added to acidify the solution to pH 5. Dextran-DVS precipitation was achieved after 300 mL of cold isopropanol was added. The gel-like precipitate was dissolved in H_2O and dialyzed using 2 kDa MWCO dialysis tubing; the dialysis solution was changed every 12 h, and the dialysis was left for 3 days. The resulting dextran-DVS solution was concentrated to a final volume of 100 mL by overnight exposure to a N_2 stream. The solution was dried and 7.5 g (yield = 74%) of lyophilized powder was obtained. A schematic detailing the entire synthesis process is shown in Figure S16.

The degree of substitution (DS) of dextran can be defined as the number of vinyl sulfone groups per 100 glucopyranose residues. The calculated DS of dextran that has been used for coating IOPs in this work is 4.6 and the calculation is based on ^{1}H NMR (Figure S17). The DS can be controlled by altering the reaction time; therefore it is possible to obtain dextran-DVS with a higher DS. However, the solubility of DVS-modified dextran was found to negatively correlate

https://dx.doi.org/10.1021/acsami.0c22185
ACS Appl. Mater. Interfaces 2021, 13, 11621−11630

with the DS, and therefore it was determined that dextran-DVS with a DS of 4.6 offered the optimal balance between solubility and functional group density.

Dextran-DVS-Coated Magnetic IOP Synthesis (IOP-DVS). Eighty-eight hundredths of a gram (5.4 mmol) of $FeCl_3$ and 0.55 g (2.7 mmol) of $FeCl_2{\cdot}4H_2O$ were dissolved in 50 mL of degassed water and heated to 80 °C under N_2. Ten milliliters of 17.5% $NH_3{\cdot}H_2O$ was quickly added to the flask while stirring at 800 rpm. The reaction was left for 1 h at 80 °C before 2 g of Dex-DVS was added. The solution was left to stir overnight before the resulting IOP-DVS particles were purified by washing with water while using a magnet to minimize particle loss. The particles were dried under a flow of N_2 gas.

Synthesis of E_3 or K_3-Conjugated Magnetic Particles (IOP-E_3/IOP-K_3). Ac-E_3GW-PEG_4-Cys or Ac-K_3GW-PEG_4-Cys was dissolved in PBS (pH 7.4) to a final concentration of 1 mM (as determined by UV−vis) and then added to 100 mg of IOP-DVS. The mixture was shaken at 600 rpm at room temperature overnight. The peptide solution was collected under an external magnetic field and the concentration of unreacted peptide was measured by UV−vis (Figure S18). The difference in peptide concentration before and after the reaction can be used to calculate the amount of peptide conjugated to the magnetic IOPs (for further details, see the Supporting Information). It was determined that 5.5 nmol peptide E_3 and 5.8 nmol peptide K_3 were conjugated to 1 mg of IOPs. The peptide-functionalized IOPs were purified by washing with H_2O under an external magnetic field. The mass of particles was clearly visible to the naked eye (Figure S19A) and TEM analysis revealed them to be nanometer sized (Figure S19B). Particles were stored in 75% EtOH to minimize bacterial growth. Before cell experiments, the particles were washed with PBS and diluted to a final concentration of 2 mg/mL, which equates to 11 μM E_3 in IOP-E_3 suspension or 11.6 μM K_3 in IOP-K_3 suspension.

Lipopeptide-Decorated Cell Sorting. Cells were seeded in a six-well plate (1×10^6 cells per well) and incubated overnight. Before trypsinization from the plate, cells were stained with CellTracker Green (5 μg/mL) or CellTracker Red (10 μg/mL) for 30 min; 3×10^5 green cells were incubated with 1 mL of 10 μM CPK_3 for 1 h and washed three times before mixing with the same amount of nonfunctionalized red cells. One-hundred microliters of IOP-E_3 was subsequently added to 1 mL of the cell mixture to facilitate formation of a coiled-coil between K_3-functionalized cells and the magnetic IOPs. A magnet was used to separate the cells that were connected to the IOPs from the remainder of the cell mixture. The cells in the supernatant were collected and cells connected to the IOPs were then washed three times with PBS before trypsin was added to digest the peptides (Figure S20 and 21) and dissociate the cells from the IOPs. After detachment, the cells were separated from the IOPs by application of an external magnetic field. Both cell populations were washed twice with PBS before being analyzed. To probe the utility of IOPs functionalized with K_3, we repeated the process above, but cells were decorated with CPE_3 and IOPs were labeled with K_3 in the same manner as described above.

Fluorescence Spectroscopy. Fluorescence measurements were performed using a Tecan Infinite M1000 plate reader. All spectra were collected with 200 μL of 2 mg/mL IOPs at room temperature in black 96-well plates. For tryptophan fluorescence measurements, excitation was performed at 275 nm and emission recorded from 450 to 310 nm.

In the IOPs fluorescent labeling assay, 200 μL of 10 μM fluo-E_3 or fluo-K_3 was added to nonfunctionalized IOPs or IOPs with a complementary coiled-coil-forming peptide. After a 1 min incubation, the IOPs were thoroughly washed and resuspended in PBS. The IOPs were transferred to a black 96-well plate and a spectrum was recorded. Excitation was performed at 488 nm and the emission spectrum was recorded between 650 and 510 nm.

Confocal Microscopy. Cell imaging was performed using a Leica SPE laser scanning confocal microscope. Cells expressing GFP, or stained with CellTracker Green or labeled with fluo-K_3/E_3 were excited with a 488 nm laser and the emission signal was detected from 495 to 530 nm. Cells stained with CellTracker Red were excited with a 532 nm laser and emission detected between 560 and 600 nm. Cells labeled with Cy5-E_3 were excited with a 635 nm laser and emission detected from 650 to 690 nm.

Flow Cytometry. All flow cytometry measurements were performed with a Guava EasyCyte 12HT Benchtop Flow Cytometer and the data was analyzed using *FlowJo* v10. The cells were suspended in PBS containing 2 mM EDTA at a concentration of approximately 500 cells/μL. Five thousand events in duplicate were collected for each measurement. A manual gating strategy can be founding in Supporting Information (Figures S4−S6 and S8−S11). Quadrant gates were used to quantify the fluorescence of Cell Tracker Red (RED-B) versus Cell Tracker Green (GRN-B) or GFP expression (GRN-B) versus cell size (FSC-A). No compensation was required for the fluorophores used.

Plasmid Constructs. A DNA fragment coding for a signal peptide sequence from the mouse IgK gene and the K_3 peptide fused to a transmembrane domain from PDGFRB, and EGFP was purchased from BaseClear (Leiden, NL) and cloned into an Acc65I and NotI digested pEBMulti-Hyg vector (Wako Pure Chemical Ind, Osaka, Japan) as described previously.[37] The DNA sequence is shown in Figure S22.

Cell Transfection and Antibiotics Selection. HeLa and NIH3T3 cells were seeded in a 12-well plate and grown to 80% confluency. One microgram of plasmid (0.2 μg/μL) and 8 μg of PEI were used per well. The cells were incubated with the DNA/PEI complex for 5 h at 37 °C and then washed with DMEM three times.

CHO cells were transfected using Lipofectamine 3000. Cells were seeded in a 24-well plate and allowed to grow to 80% confluency. One-half a microgram of plasmid DNA (0.2 μg/ μL) and 1.5 μL of Lipofectamine 3000 were used per well. Cell were incubated at 37 °C for 5 h before washing the cells with DMEM for three times.

After transfection, all cells were grown for 3 days. Hygromycin B was used to enrich successfully transfected cells. After 2 weeks of antibiotic selection, the percentage of GFP-positive cells was found to stop increasing, presumably because the cells acquired resistance to the antibiotic. At this point, the GFP-expressing cells comprised approximately 10% of the total cell population.

MACS with GFP-K_3-Expressed Cells. Before MACS, GFP-K_3-expressing cells were subcultured for at least two generations. The cells were subsequently detached from the cell culture plate using EDTA (2 mM in PBS) and dispersed by thorough pipetting. Cell sorting was performed by utilizing 1 mL of cell suspension containing 1×10^6 GFP-K_3 expressing cells. One hundred microliters of IOP-E_3 suspension was subsequently added to enable coiled-coil formation between the K_3 peptide on the cell membrane and the E_3 peptide attached to the IOPs. A magnet was then used to separate the cells that were connected to the IOPs from the other cells in the mixture. Cells connected to the IOPs were washed with PBS three times and trypsin was then added to dissociate the cells from the IOPs. After detachment, the cells and IOPs were separated by application of an external magnetic field.

Transmission Electron Microscopy. A 10 μL droplet of the IOPs was placed on a Forvar/carbon grid (200 mesh) and left for 10 min. The excess solution was blotted off and the grid was left to air-dry. Images were obtained used a JEM1400 plus (JEOL) microscope operating at 80 kV. The microscope was fitted with a CCD camera.

■ ASSOCIATED CONTENT

Supporting Information

The Supporting Information is available free of charge at https://pubs.acs.org/doi/10.1021/acsami.0c22185.

Confocal microscopy images of cell labeling experiments and MACS with CHO and NIH3T3 cells, FACS analysis, LCMS data, ^{1}H NMR data for the Dex-DVS polymer and an explanation of how the polymer substitution degree was calculated, a calculation for the determination of peptide concentration on the IOPs, IOP characterization data, trypsin degradation experiments, and the DNA sequence of the K_3-TMD-GFP gene construct (PDF)

https://dx.doi.org/10.1021/acsami.0c22185
ACS Appl. Mater. Interfaces 2021, 13, 11621−11630

AUTHOR INFORMATION

Corresponding Authors

Alexander Kros − *Department of Supramolecular & Biomaterials Chemistry, Leiden Institute of Chemistry, Leiden University, Leiden 2333 CC, The Netherlands;* orcid.org/0000-0002-3983-3048; Email: a.kros@chem.leidenuniv.nl

Aimee L. Boyle − *Department of Macromolecular Biochemistry, Leiden Institute of Chemistry, Leiden University, Leiden 2333 CC, The Netherlands;* orcid.org/0000-0003-4176-6080; Email: a.l.boyle@chem.leidenuniv.nl

Authors

Meng-Jie Shen − *Department of Supramolecular & Biomaterials Chemistry, Leiden Institute of Chemistry, Leiden University, Leiden 2333 CC, The Netherlands*

René C.L. Olsthoorn − *Department of Supramolecular & Biomaterials Chemistry, Leiden Institute of Chemistry, Leiden University, Leiden 2333 CC, The Netherlands*

Ye Zeng − *Department of Supramolecular & Biomaterials Chemistry, Leiden Institute of Chemistry, Leiden University, Leiden 2333 CC, The Netherlands*

Thomas Bakkum − *Department of Bio-organic Synthesis, Leiden Institute of Chemistry, Leiden University, Leiden 2333 CC, The Netherlands*

Complete contact information is available at: https://pubs.acs.org/10.1021/acsami.0c22185

Author Contributions

All authors contributed to the experimental design. R.C.L.O. designed and constructed the plasmid. M.S. and Y.Z. performed the cell transfection experiment. M.S. performed all other experiments. T.B. assisted with flow cytometry. All authors analyzed the data. The manuscript was written by M.S. and A.L.B. with contributions from the other authors.

Funding

M.S. and Y.Z. acknowledge the support of the Chinese Scholarship Council (CSC). A.K. acknowledges the support of an NWO (Netherlands Organization for Scientific Research) VICI grant (724.014.001).

Notes

The authors declare no competing financial interest.

REFERENCES

(1) Chen, P.; Huang, Y. Y.; Hoshino, K.; Zhang, X. Multiscale immunomagnetic enrichment of circulating tumor cells: from tubes to microchips. *Lab Chip* **2014**, *14*, 446−458.

(2) Di Corato, R.; Bigall, N. C.; Ragusa, A.; Dorfs, D.; Genovese, A.; Marotta, R.; Manna, L.; Pellegrino, T. Multifunctional nanobeads based on quantum dots and magnetic nanoparticles: synthesis and cancer cell targeting and sorting. *ACS Nano* **2011**, *5*, 1109−1121.

(3) Geens, M.; Van de Velde, H.; De Block, G.; Goossens, E.; Van Steirteghem, A.; Tournaye, H. The efficiency of magnetic-activated cell sorting and fluorescence-activated cell sorting in the decontamination of testicular cell suspensions in cancer patients. *Hum. Reprod.* **2007**, *22*, 733−742.

(4) Saliba, A. E.; Saias, L.; Psychari, E.; Minc, N.; Simon, D.; Bidard, F. C.; Mathiot, C.; Pierga, J. Y.; Fraisier, V.; Salamero, J.; Saada, V.; Farace, F.; Vielh, P.; Malaquin, L.; Viovy, J. L. Microfluidic sorting and multimodal typing of cancer cells in self-assembled magnetic arrays. *Proc. Natl. Acad. Sci. U. S. A.* **2010**, *107*, 14524−14529.

(5) Gil, M.; Sar-Shalom, V.; Melendez Sivira, Y.; Carreras, R.; Checa, M. A. Sperm selection using magnetic activated cell sorting (MACS) in assisted reproduction: a systematic review and meta-analysis. *J. Assist. Reprod. Genet.* **2013**, *30*, 479−485.

(6) Fong, C. Y.; Peh, G. S.; Gauthaman, K.; Bongso, A. Separation of SSEA-4 and TRA-1−60 labelled undifferentiated human embryonic stem cells from a heterogeneous cell population using magnetic-activated cell sorting (MACS) and fluorescence-activated cell sorting (FACS). *Stem Cell Rev. Rep.* **2009**, *5*, 72−80.

(7) Schriebl, K.; Lim, S.; Choo, A.; Tscheliessnig, A.; Jungbauer, A. Stem cell separation: a bottleneck in stem cell therapy. *Biotechnol. J.* **2010**, *5*, 50−61.

(8) Kim, H.; Kim, M. S.; Wee, G.; Lee, C. I.; Kim, H.; Kim, J. S. Magnetic separation and antibiotics selection enable enrichment of cells with ZFN/TALEN-induced mutations. *PLoS One* **2013**, *8*, No. e56476.

(9) Ren, C.; Xu, K.; Segal, D. J.; Zhang, Z. Strategies for the Enrichment and Selection of Genetically Modified Cells. *Trends Biotechnol.* **2019**, *37*, 56−71.

(10) Bacon, K.; Lavoie, A.; Rao, B. M.; Daniele, M.; Menegatti, S. Past, Present, and Future of Affinity-based Cell Separation Technologies. *Acta Biomater.* **2020**, *112*, 29−51.

(11) Plouffe, B. D.; Murthy, S. K.; Lewis, L. H. Fundamentals and application of magnetic particles in cell isolation and enrichment: a review. *Rep. Prog. Phys.* **2015**, *78*, 016601.

(12) Miltenyi, S.; Muller, W.; Weichel, W.; Radbruch, A. High gradient magnetic cell separation with MACS. *Cytometry* **1990**, *11*, 231−238.

(13) Molday, R. S.; Yen, S. P.; Rembaum, A. Application of magnetic microspheres in labelling and separation of cells. *Nature* **1977**, *268*, 437−438.

(14) Moore, L. R.; Zborowski, M.; Sun, L.; Chalmers, J. J. Lymphocyte fractionation using immunomagnetic colloid and a dipole magnet flow cell sorter. *J. Biochem. Biophys. Methods* **1998**, *37*, 11−33.

(15) Schmitz, B.; Radbruch, A.; Kummel, T.; Wickenhauser, C.; Korb, H.; Hansmann, M. L.; Thiele, J.; Fischer, R. Magnetic activated cell sorting (MACS)–a new immunomagnetic method for megakaryocytic cell isolation: comparison of different separation techniques. *Eur. J. Haematol.* **1994**, *52*, 267−275.

(16) Weil, B. D.; Jenkins, M. J.; Uddin, S.; Bracewell, D. G.; Wellings, D.; Farid, S. S.; Veraitch, F. An integrated experimental and economic evaluation of cell therapy affinity purification technologies. *Regener. Med.* **2017**, *12*, 397−417.

(17) Chalmers, J. J.; Xiong, Y.; Jin, X.; Shao, M.; Tong, X.; Farag, S.; Zborowski, M. Quantification of non-specific binding of magnetic micro- and nanoparticles using cell tracking velocimetry: Implication for magnetic cell separation and detection. *Biotechnol. Bioeng.* **2010**, *105*, 1078−1093.

(18) Moore, D. K.; Motaung, B.; du Plessis, N.; Shabangu, A. N.; Loxton, A. G. Isolation of B-cells using Miltenyi MACS bead isolation kits. *PLoS One* **2019**, *14*, No. e0213832.

(19) Farrell, E.; Wielopolski, P.; Pavljasevic, P.; van Tiel, S.; Jahr, H.; Verhaar, J.; Weinans, H.; Krestin, G.; O'Brien, F. J.; van Osch, G.; Bernsen, M. Effects of iron oxide incorporation for long term cell tracking on MSC differentiation in vitro and in vivo. *Biochem. Biophys. Res. Commun.* **2008**, *369*, 1076−1081.

(20) Meinhardt, K.; Kroeger, I.; Abendroth, A.; Muller, S.; Mackensen, A.; Ullrich, E. Influence of NK cell magnetic bead isolation methods on phenotype and function of murine NK cells. *J. Immunol. Methods* **2012**, *378*, 1−10.

(21) Mahmoudi, M.; Azadmanesh, K.; Shokrgozar, M. A.; Journeay, W. S.; Laurent, S. Effect of nanoparticles on the cell life cycle. *Chem. Rev.* **2011**, *111*, 3407−3432.

(22) Van de Walle, A.; Perez, J. E.; Abou-Hassan, A.; Hémadi, M.; Luciani, N.; Wilhelm, C. Magnetic nanoparticles in regenerative medicine: what of their fate and impact in stem cells? *Mater. Today Nano* **2020**, *11*, 100084.

(23) Crick, F. H. C. Is α-Keratin a Coiled Coil? *Nature* **1952**, *170*, 882−883.

(24) Woolfson, D. N. The design of coiled-coil structures and assemblies. *Adv. Protein Chem.* **2005**, *70*, 79−112.

(25) Fletcher, J. M.; Boyle, A. L.; Bruning, M.; Bartlett, G. J.; Vincent, T. L.; Zaccai, N. R.; Armstrong, C. T.; Bromley, E. H.; Booth, P. J.;

Brady, R. L.; Thomson, A. R.; Woolfson, D. N. A basis set of de novo coiled-coil peptide oligomers for rational protein design and synthetic biology. *ACS Synth. Biol.* **2012**, *1*, 240−50.
(26) Harbury, P. B.; Zhang, T.; Kim, P. S.; Alber, T. A switch between two-, three-, and four-stranded coiled coils in GCN4 leucine zipper mutants. *Science* **1993**, *262*, 1401−1407.
(27) Apostolovic, B.; Danial, M.; Klok, H. A. Coiled coils: attractive protein folding motifs for the fabrication of self-assembled, responsive and bioactive materials. *Chem. Soc. Rev.* **2010**, *39*, 3541−3575.
(28) Beesley, J. L.; Woolfson, D. N. The de novo design of alpha-helical peptides for supramolecular self-assembly. *Curr. Opin. Biotechnol.* **2019**, *58*, 175−182.
(29) Robson Marsden, H.; Kros, A. Self-Assembly of Coiled Coils in Synthetic Biology: Inspiration and Progress. *Angew. Chem., Int. Ed.* **2010**, *49*, 2988−3005.
(30) Wu, Y. Y.; Collier, J. H. alpha-Helical coiled-coil peptide materials for biomedical applications. *Wiley Interdis. Rev. Nanomed. Nanobiotechnol.* **2017**, *9*, No. e1424.
(31) Litowski, J. R.; Hodges, R. S. Designing heterodimeric two-stranded alpha-helical coiled-coils. Effects of hydrophobicity and alpha-helical propensity on protein folding, stability, and specificity. *J. Biol. Chem.* **2002**, *277*, 37272−37279.
(32) Zope, H. R.; Versluis, F.; Ordas, A.; Voskuhl, J.; Spaink, H. P.; Kros, A. In vitro and in vivo supramolecular modification of biomembranes using a lipidated coiled-coil motif. *Angew. Chem., Int. Ed.* **2013**, *52*, 14247−14251.
(33) Versluis, F.; Voskuhl, J.; van Kolck, B.; Zope, H.; Bremmer, M.; Albregtse, T.; Kros, A. In situ modification of plain liposomes with lipidated coiled coil forming peptides induces membrane fusion. *J. Am. Chem. Soc.* **2013**, *135*, 8057−8062.
(34) Yang, J.; Bahreman, A.; Daudey, G.; Bussmann, J.; Olsthoorn, R. C. L.; Kros, A. Drug Delivery via Cell Membrane Fusion Using Lipopeptide Modified Liposomes. *ACS Cent. Sci.* **2016**, *2*, 621−630.
(35) Crone, N. S. A.; Kros, A.; Boyle, A. L. Modulation of Coiled-Coil Binding Strength and Fusogenicity through Peptide Stapling. *Bioconjugate Chem.* **2020**, *31*, 834−843.
(36) Yu, Y.; Chau, Y. One-step "click" method for generating vinyl sulfone groups on hydroxyl-containing water-soluble polymers. *Biomacromolecules* **2012**, *13*, 937−942.
(37) Yang, J.; Shimada, Y.; Olsthoorn, R. C.; Snaar-Jagalska, B. E.; Spaink, H. P.; Kros, A. Application of Coiled Coil Peptides in Liposomal Anticancer Drug Delivery Using a Zebrafish Xenograft Model. *ACS Nano* **2016**, *10*, 7428−74235.

https://dx.doi.org/10.1021/acsami.0c22185
ACS Appl. Mater. Interfaces 2021, 13, 11621−11630